WPMAT-PR(17) 18876

A Łestan et al.

The role of tungsten phases formation during tungsten metal powder consolidation by FAST: Implications for high-temperature applications

Preprint of Paper to be submitted for publication in
Materials Characterization

This work has been carried out within the framework of the EUROfusion Consortium and has received funding from the Euratom research and training programme 2014-2018 under grant agreement No 633053. The views and opinions expressed herein do not necessarily reflect those of the European Commission.

The role of tungsten phases formation during tungsten metal powder consolidation by FAST: Implications for high-temperature applications

A. Šestan[1,2], P. Jenuš[3], S. Novak[3], J. Zavašnik[1], M. Čeh[1,2,3]

[1] Centre for Electron Microscopy and Microanalysis, Jožef Stefan Institute, Ljubljana, Slovenia

[2] Jožef Stefan International Postgraduate School, Ljubljana, Slovenia

[3] Department for Nanostructured Materials, Jožef Stefan Institute, Ljubljana, Slovenia

Abstract

Tungsten is a candidate material for the demonstration fusion power plant DEMO. To ensure high density and structural stability, Field-Assisted Sintering Technique (FAST) is proposed as a consolidation method. This study discusses the formation of phases during sintering of tungsten by the FAST. Scanning electron microscopy, X-ray diffraction and transmission electron microscopy were used to evaluate the microstructure in tungsten-based materials. The results of microscopic examinations revealed the *in-situ* formation of tungsten oxide and a formation of tungsten carbide shell around tungsten core. Tungsten carbide-rich shell is formed due to the carbon diffusion from the graphite die used in the FAST into tungsten at high temperatures. In contrast to easy removal of tungsten carbide shell by mechanical grinding, the formation of tungsten oxide in the W-matrix can influence the performance of such material when used as plasma-facing material in the fusion reactor. High-temperature experiments at 1873 K showed that tungsten-oxide phase starts to evaporate, which results in material degradation and formation of voids and surface blisters.

Keywords: fusion, FAST, tungsten, tungsten oxide, electron microscopy, microstructure

1. Introduction

It is expected that fusion power will significantly contribute to clean and safe energy supply for future generations [1]. To achieve high efficiency and safe operation of future fusion power plants, researchers are putting much effort into the selection and optimisation of suitable structural materials capable of withstanding the extreme conditions within the fusion reactor [2]. One of the key challenges is to find a suitable plasma-facing material for the divertor [3], which will be exposed to very high transient thermal events, neutron irradiation and helium and hydrogen isotopes irradiation. Tungsten (W) is a promising material for fusion applications due to its high melting point (3717 K), high thermal conductivity (175 $Wm^{-1}K^{-1}$ at 298 K), low thermal expansion coefficient (4.32 10^{-6} K^{-1} at 298 K), low sputtering yield and low tritium retention [4, 5]. Its main disadvantage is relatively poor oxidation resistance; hence, hydrogen reduction atmosphere or vacuum conditions during sintering are required. Vacuum-assisted sintering is used to provide oxygen-free atmosphere, reduced adsorption of oxygen on the surface of starting W powder which should consequently result in a defect-free single phase tungsten microstructure with improved mechanical properties such as hardness, yield strength and ultimate tensile strength [4]. Densification of W by a conventional solid-state sintering process in reductive atmosphere requires high temperatures and lengthy sintering time due to high melting point of W. However, this often results in W microstructure with included porosity and exaggerated grain growth which lowers mechanical strength at elevated temperatures and also significantly lowers recrystallisation temperature [2, 7, 8]. To reduce these adverse effects and to improve the material density, additional processing such as forging, swaging or rolling is required [2, 6].

Recently, an alternative sintering method, named *Field-Assisted Sintering Technique* (FAST), was proposed to improve the sinterability of W and to minimise grain growth phenomenon during the sintering process. FAST offers vacuum environment under uniaxial compression and rapid consolidation of powders, which are heated directly by a low-voltage high-intensity current flowing through the die and through the sample itself [6, 9]. Short sintering time, an order of magnitude shorter than in conventional sintering prevents or minimises tungsten grain growth during the sintering [6, 9]. On the other hand, apart from the formation of the external shell from the FAST graphite tooling setup [5], secondary phases, if formed during the FAST sintering of tungsten, are usually nano-sized and scarce; therefore, their detection and identification may be rather difficult. Nevertheless, the identification of such phases and their structural stability at elevated temperatures is a prerequisite for materials used in fusion plasma-applications [2]. The “burst out” of the plasma (plasma disruption and ELMs) during fusion reactor operation is expected to be frequent, and most of the plasma thermal energy will be discarded on the divertor [2]. The expected temperature gradient

within the limited volume near the loaded material surface during plasma disruption will be in the range of hundreds to several thousand Kelvin. Currently suggested reinforcing secondary phases (such as La_2O_3 [6]) in W-based materials have a far lower melting point than tungsten, so during disruptions this can lead to early melting and increased evaporation, causing the formation of pores and depleted surface layer [2]. Melting of the material surface will cause increased material degradation, which will significantly limit the lifetime of the material [2]. In the present study, we first characterise and then discuss the formation of secondary phases formed during the FAST sintering of W powder, carried out at 2173 K and 60 MPa. To investigate the high-temperature structural stability of the phases formed during FAST, we performed the additional thermal treatment at 1873 K to investigate how the secondary phase volatilisation affects the microstructure of W.

2. Materials and Methods

2.1 Sample preparation

A commercially available 99.9 % pure tungsten powder with average grain size of 0.7 µm (MPO7R; Global Tungsten & Powder, USA) was used as a starting material. For sintering experiments, we employed field-assisted sintering device (FAST; Dr SINTER SPS SYNTEX 3000, Fuji Electronic Industrial, Japan). The W powder was loaded into a graphite die (inner diameter 16 mm), while additional 0.3 mm graphite foil was used to prevent adhesion of the W on the die wall (Fig. 1). Prior to sintering the FAST chamber was thoroughly purged with N_2 (99.996 % pure) and evacuated (0.3 mbar - 0.5 mbar). The samples were sintered at an applied pressure of 60 MPa with a heating rate of 100 K/min. To investigate the effect on microstructure, sintering time was 1 minute (sample W1) and 10 minutes (W10).

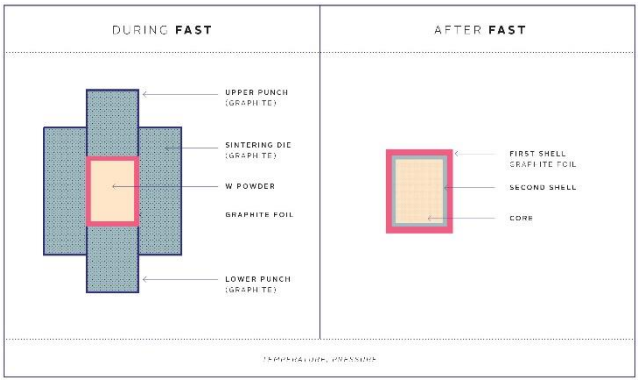

Figure 1: Schematic representation of the FAST die and sample during and after consolidation.

To verify the structural stability of FAST sintered W at high temperatures, additional thermal treatments were performed in a high-temperature vacuum furnace (Astro, Thermal Technology LLC., USA) at 1873 K for 30 min or 24 h with 5 K/min heating rate. Before each experiment, the furnace was thoroughly purged with Ar (99.998 % pure) and evacuated (0.2 mbar - 0.35 mbar). The samples' surface was mechanically ground and polished before additional thermal treatments. To prevent carbon contamination, tungsten die was used.

2.2. Material characterization

For the characterization of as-received tungsten powder, we used X-ray powder diffraction analysis, using CuKα radiation at room temperature (XRD; AXS D4 Endeavor, Bruker AXS GmbH, Germany), while size and morphology of W crystallites were assessed with a field-emission scanning electron microscope (FE-SEM, JSM-7600F, Jeol Inc., Japan).

After FAST treatment, the sintered samples were ground to remove outer contamination layer, induced by graphite die used during FAST and were analysed by XRD to evaluate the phase-composition. Microstructural observation and chemistry of the synthesised product were assessed by FE-SEM. The chemical composition of the secondary phases was studied by energy-dispersive X-ray spectroscopy (EDS; X-Max, Oxford Instruments plc., UK), while their microstructure and crystallinity were studied by electron-backscatter diffraction (EBSD; Nordlys II, Oxford Instruments plc., UK). Samples for FE-SEM and EBSD analyses were prepared by mechanical grinding and polishing. To achieve an adequate surface quality and to remove a mechanically-induced damaged layer, a final polishing with 5 vol.% H_2O_2 solution in colloidal silica was applied. Due to the detection limit of the XRD technique [7], co-formed secondary phases were additionally investigated by transmission electron microscopy (TEM, JEM-2100, Jeol Inc., Japan) and scanning transmission electron microscopy (S/TEM, JEM-2010F, Jeol Inc., Japan). Prior to TEM observation, the samples were prepared by conventional mechanical thinning and subsequently etched in ion-mill using high-energy Ar^+ until electron transparency (PIPS 691, Gatan Inc., USA).

3. Results and discussion

3. 1. Phase identification

Grain size and morphology of the starting W powder were investigated by FE-SEM. From secondary electrons images (SEI) we assessed that the size of the starting tungsten particles was < 1 µm. Tungsten particles tend to form larger agglomerates (Fig. 2a). W particles exhibit an irregular shape with faceted edges. XRD diffractogram of initial powder corresponds to pure tungsten with the body-cantered cubic structure (a = 3.165 Å, Im-3m SG: 229) [8] (Fig. 2b). Very narrow diffraction peaks indicate well-crystalline material and particle size in the micron range.

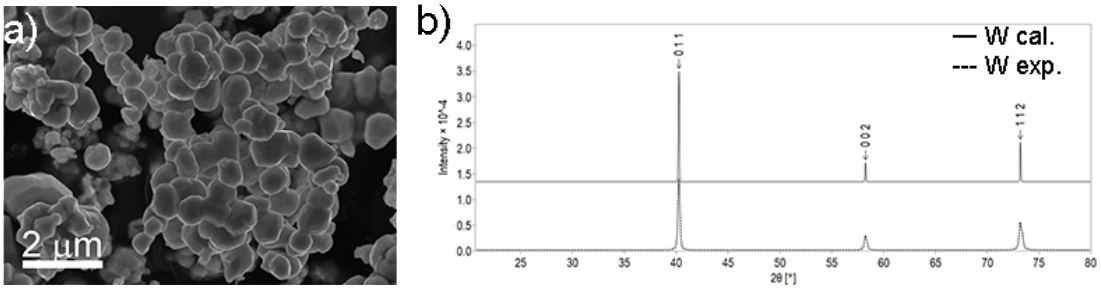

Figure 2: a) SEI image of starting W powder, b) comparison of an experimental X-ray diffractogram of starting W powder (W exp.) and calculated W pattern (W cal.).

During the FAST consolidation of the W powder, carbon diffuses from the graphite foil and die into the sample, forming two additional layers on the surface of the sintered specimen as shown in Figure 1.

While the first layer is a thin graphite foil from the wrapping that can be removed easily, the second layer, which has a different texture, is a hard, thick crust, enclosing the W sintered sample (Fig. 3a1)). XRD analysis (Fig. 3a) revealed that this second layer is a mixture of W [8] and $W_2C_{0.85}$ [9]. The investigation of the fractured sample showed that this carburised layer is approximately 200 µm thick (Fig. 3a1), and that it is formed during sintering due to direct contact of the specimen with the graphite-foil and graphite die; this carburised layer is assumed to grow in a parabolic manner with time [5]. The thickness of this tungsten carbide-rich layer is important regarding the further sample preparation. Therefore, before any microstructure characterisation, we have to remove this remaining processing artefact to avoid possible misinterpretation of the results.

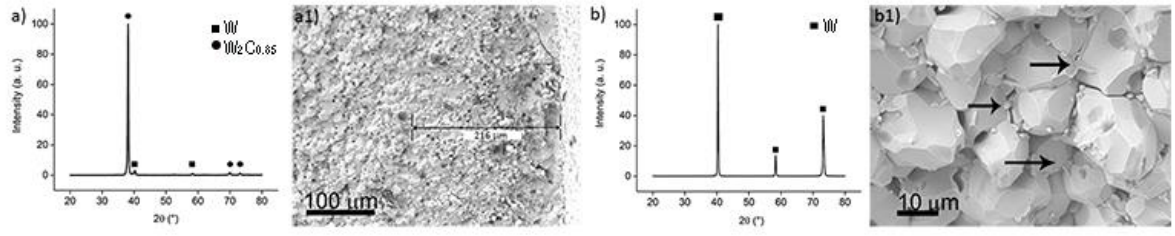

Figure 3: a) Experimental X-ray diffractogram of the second layer, a1) fractured W1 sintered sample after the graphite foil has been removed from the surface, showing outer tungsten carbide rich layer surrounding the W-core, b) X-ray diffractogram of the W-core and b1) W-core with a secondary phase (marked with arrows).

After removal of the carburised layer, a close-up inspection of the pellets' core revealed W-matrix grains with a small fraction of secondary phase in the shape of small grains along grain boundaries of W grains (Fig. 3b1). An attempt to identify the unknown phase by XRD analysis was not successful, as the only phase detected is the bcc-W of the matrix [8], meaning that the overall concentration of the secondary phase is below the detection limit of the XRD (Fig. 3b). In an attempt to increase grain growth of the observed unknown phase, we extended the FAST sintering time to 10 minutes, while other conditions (P = 60 MPa, T = 2173 K, r=100K/min) remained unaltered; again the carbide layer was ground away, and the microstructure of the tungsten pellet core was investigated by SEM. The prolonged sintering time at high temperature indeed resulted in merging and growth of neck-shaped unknown phase, which made it possible to identify it as an oxygen-rich W phase by semi-quantitative EDS mapping, as shown in Figure 4. To avoid contamination and alteration of the sample, the surface was Ar^+ etched before analysis.

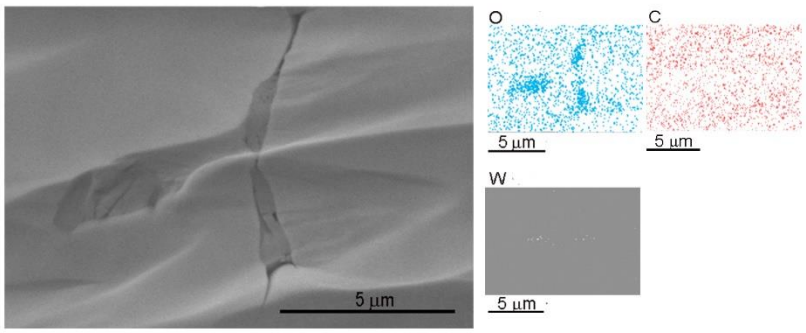

Figure 4: a) Grain boundary secondary phase observed in the W10 sample (BEI-SEM) with the corresponding EDS mapping for O, C and W.

The morphology and crystal structure of this unknown oxide-rich W phase was further investigated by TEM. The initial overview of the W10 sample using bright-field TEM imaging (Fig. 5a, b) revealed the presence of individual W grains with a size of approximately 10 µm. No visible planar defects could be observed within the W grains (Fig. 6a). On the other hand, the oxygen-rich W phase exhibits ceramic-like Ar^+ etching patterns [10], which already makes it easy to distinguish it from the W grains. In general, two different types of oxygen-rich W phase could be observed; namely intergranular single-crystal oxygen-rich W phase with well-developed morphology and size of about 1 µm (Fig. 5a) and neck-like polycrystalline oxygen-rich W phase between individual tungsten grains (Fig. 5b), similar as observed already by SEM (Fig. 3). Both phases, namely W grains and the oxygen-rich W phase, can be even easier distinguished using HAADF STEM imaging (Fig. 5c, d), where the contrast in the image is contributed mainly by high angle, incoherently scattered electrons and thus the contrast of individual phase is approximately proportional to Z^2 [11] [12].

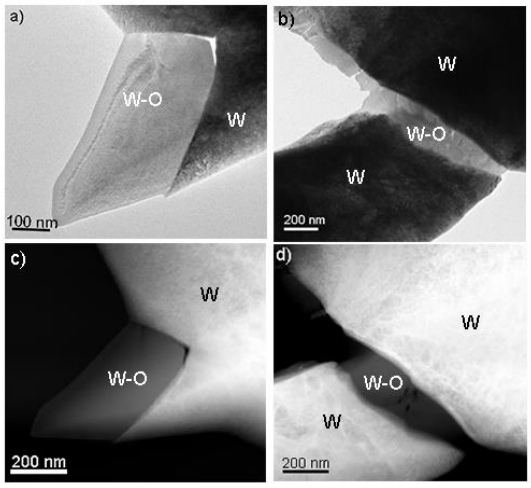

Figure 5: (a, b) Bright-field TEM micrographs of W10 sample showing W grains and oxygen-rich W phase. The latter can be observed as a standalone crystalline phase or as neck-like grain boundary phase. (c, d) HAADF STEM micrographs are showing the same region as in a and in b. The difference

in contrast between W grains and oxygen-rich W phase is largely increased due to reduced average atomic number Z of the oxygen-rich W phase.

Crystal structure of W-matrix was determined from selected area electron diffraction pattern (SAEDP). The diffraction pattern corresponds to W bcc (Im3m (SG: 229) (Fig. 6 a1) [8], which is in agreement with XRD analyses obtained from the starting powder and after the FAST treatment. The preservation of the W crystal structure and the absence of usually present planar defects [13] can be attributed to rapid sintering and a relatively small size of the tungsten grains. Additionally, due to the absence of rolling and forging, the mechanically induced strain and stress were preferentially compensated along the grain-boundaries between tungsten grains as opposed to the formation of planar defects.

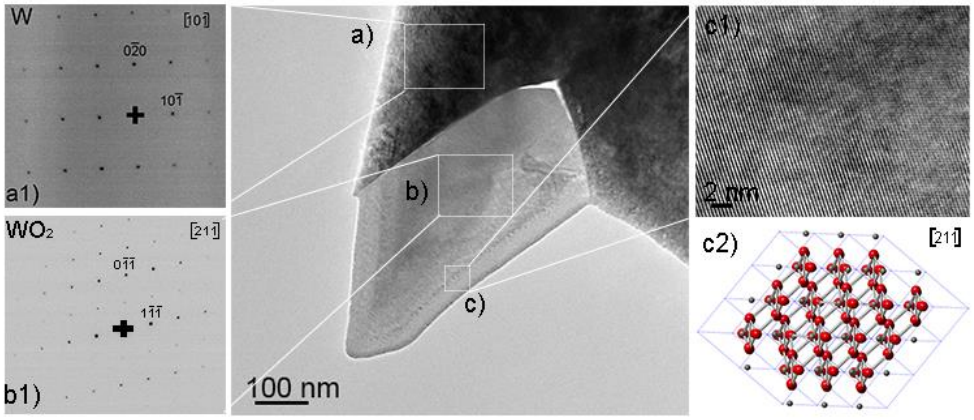

Figure 6: BF-TEM micrograph and corresponding electron diffraction patterns (SAEDP) of the bcc W-matrix (a1) and monoclinic WO_2 (b1); HR-TEM of the WO_2 and corresponding structure model in the same orientation (c2).

The crystal structure of the oxygen-rich W phase was determined to be a simple monoclinic WO_2 $P2_1/c$ (SG: 14) structure (Fig. 6b1) [14] by interpretation of single-crystal SAED patterns, recorded in different orientations. Based on our structure determination we were able to prepare a database for electron backscatter diffraction (EBSD) analyses as a way of phase recognition. Since the signal in the EBSD analysis depends on the crystal structure of the investigated grain, the resulting compositional map presents unique and precise information on spatial distribution of both W and WO_2 phases in the sample. Since the differentiation of the phases is based on two different structures: namely cubic W and monoclinic WO_2, the resulting band contrast map allocates the grains and grain boundaries easily (Fig. 7a), while phase composition (Fig. 7b) shows the presence of WO_2 phase around W grains. It is necessary to mention that the preparation of the surface for EBSD analysis is crucial, since the diffracted electrons, forming the signal, originate only from few nm thin surface region of W. With grinding and polishing mechanically induced deformation layer is formed, which must be removed by final finish polishing using chemical etchants, like H_2O_2. In the two phases system (W and WO_2), the main problem is preferential etching of oxide-rich W phase [5], which strongly affect the results. In

work presented here the mechanically damaged layer was removed by etching with H_2O_2 for 15 min, which already removed most of the intra-granular WO_2 grains, but preserved most of the neck-like shaped WO_2 around W grains.

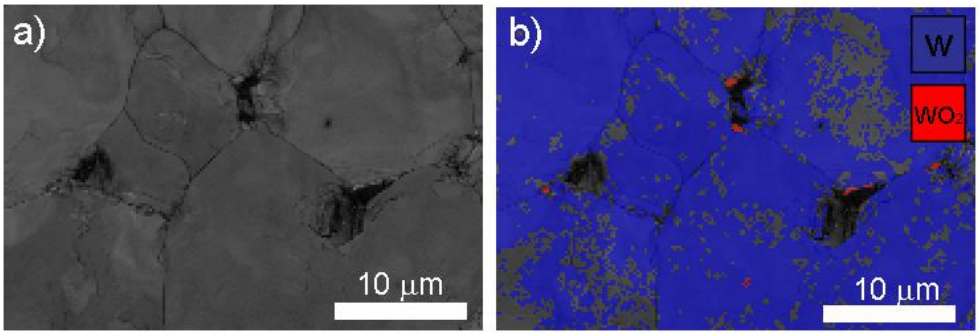

Figure 7: Electron backscatter diffraction images of a) band contrast map, b) phase composition with distribution for cubic W (blue) and monoclinic WO_2 phase (red).

3.2 High-temperature structures stability

To assess the suitability of the FAST sintered W as a material for fusion reactor divertor, we performed the high-temperature structure-stability test. The formed WO_2 phase has a much lower melting point compared to pure W (WO_2 = 1803 K, W = 3695 K [2]). Therefore, the temperature was set to 1873 K to determine the influence of WO_2 decomposition on bulk material. In the first experiment, the FAST sintered sample was held for 30 min at 1873 K in vacuum-furnace. At this temperature, the recrystallisation of mechanically induced deformation layer started (Fig. 8a). During this process, a set of defect-free smaller grains are formed while outlines of initial grain are still visible. The miss-orientation of individual grains is visible due to the channelling effect on backscattered electron images (Fig. 8a). After 30 min of high-temperature exposure, the material surface starts to degrade; voids are formed at the W grain-boundaries and blisters bursting on the surface (Fig. 8b), where the tungsten oxide grains were positioned before annealing (Fig. 8c).

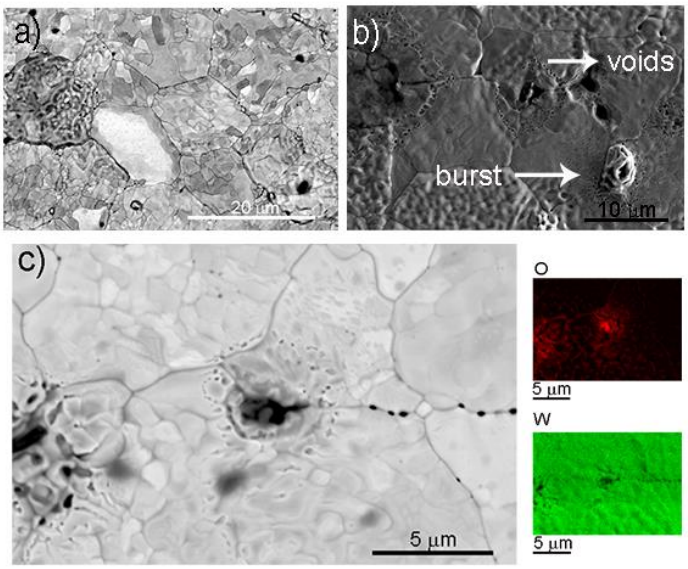

Figure 8: a) Electron backscatter image of the mechanical induce deformation layer after aging. b) Voids and outbursting are visible on the grain boundary of the W sample after annealing (SEI-SEM) with c) the corresponding EDS mapping for O and W.

In the second high-temperature experiment, the annealing time was increased from 30 min to 24 h at 1873 K. The main difference was the total absence of W-oxides; apparently, tungsten (II) oxide is highly volatile (Fig. 9) [12]. Such evaporation of tungsten oxides can contaminate the plasma system, and chemical reactions may occur possibly leading to fire or explosions [15].

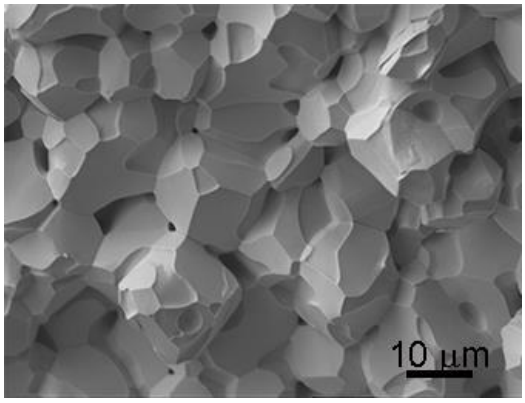

Figure 9: SEM micrograph of the fractured surface of the sample after ageing at 1873 K for 24h.

4. Conclusion

In-situ secondary phases formation during tungsten powder consolidation in FAST must be taken into account when considering fusion applications. Due to the low concentration of secondary phases in the sample, the information obtained from imaging, electron diffraction and microanalysis have to be combined to allow detailed insight into the properties and behaviour of such composites. The two-phase system was identified in the FAST sintered W samples via structural and chemical characterisation performed by SEM and TEM, and the corresponding cubic W and monoclinic WO_2 structures were determined. In-situ formation of the secondary phase, WO_2, can be attributed to the level of impurities (mainly oxygen content) in the starting W powder and residual oxygen in the furnace. In the FAST furnace, the presence of high current and magnetic fields [4] may affect phase transformation temperature, nucleation and grain growth rates and deformation behaviours of material, leading to morphological differences of WO_2 (e.g. intergranular single-crystal WO_2 and neck-like polycrystalline W-oxide).

During phase-stability tests at 1873 K, the WO_2 phase formed in W-matrix starts to evaporate. At holding times higher than 30 minutes, the material' degradation starts. Namely, blisters and voids form at the positions of WO_2 grains. With the holding time of 24 hours, a complete evaporation of WO_2 was observed.

The presence of tungsten oxide phases in the FAST consolidated tungsten can enhance the degradation of the consolidates under operation regime in the fusion reactor. Thus, to improve the performance of the tungsten processed by FAST, it is necessary to prevent the formation of tungsten oxide either by pre-processing of initial tungsten powder by H_2 reduction at atmospheric pressure [16] or by reducing oxygen content in a vacuum by the use of carbon deoxidation [4].

ACKNOWLEDGEMENT

This work has been carried out within the framework of the EUROfusion Consortium and has received funding from the Euratom research and training programme 2014-2018 under grant agreement No 633053. The views and opinions expressed herein do not necessarily reflect those of the European Commission.

References

[1] D. Maisonnier, D. Campbell, I. Cook, L. Di Pace, L. Giancarli, J. Hayward, A. Li Puma, M. Medrano, P. Norajitra, P. Sardain, M. Q. Tran and D. Ward, "Power plant conceptual studies in Europe," *Nuclear Fusion,* vol. 47, no. 11, pp. 1524-1532, 2001.

[2] G. Pintsuk, Comprehensive Nuclear Materials 4.17 - Tungsten as a Plasma-Facing Material, vol. 4, R. J. M. Konings, Ed., Oxford: Elsevier, 2012, pp. 551–581.

[3] A. S. Kukushkin, H. D. Pacher, G. Janeschitz, A. Loarte, D. P. Coster, G. Matthews, D. Reiter, R. Schneider and V. Zhogolev, "Basic divertor operation in ITER-FEAT," *Nuclear Fusion,* vol. 42, pp. 187-191, 2002.

[4] Z. Z. Fang, Sintering of Advanced Materials, Elsevier Science, 2010.

[5] G. Lee, J. McKittrick, E. Ivanov and . E. A. Olevsky, "Densification mechanism and mechanical properties of tungsten powder consolidated by spark plasma sintering," *International Journal of Refractory Metals and Hard Materials,* vol. 61, no. Complete, pp. 22-29, 2016.

[6] A. Muñoz, M. A. Monge, B. Savoini, M. E. Rabanal, G. Garces and R. Pareja, "La_2O_3-reinforced W and W–V alloys produced by hot isostatic pressing," *Journal of Nuclear Materials,* vol. 417, no. 1-3, pp. 508-511, 2011.

[7] B. D. Cullity, "Elements Of X-Ray Diffraction," *Journal of Chemical Education,* vol. 34, no. 4, pp. A 178, 1957.

[8] L. S. Dubrovinsky and S. K. Saxena, "Thermal expansion of periclase (MgO) and tungsten (W) to melting temperatures," *Physics and Chemistry of Minerals,* vol. 24, no. 8, pp. 547-550, 1997.

[9] A. Harsta, S. Rundqvist and J. O. Thomas, "A neutron powder diffraction study of W_2C," *Acta Chemica Scandinavia,* vol. A 32, pp. 891-892, 1987.

[10] L. Huang, L. Jiang, T. D. Topping, C. Dai, X. Wang, R. Carpenter, C. Haines and J. M. Schoenung, "In situ oxide dispersion strengthened tungsten alloys with high compressive strength and high strain-to-failure," *Acta Materialia,* vol. 122, pp. 19-31, 2017.

[11] R. Brydson and L. M. Brown, "Development of STEM," in *In Aberration-Corrected Analytical*, Chichester, John Wiley & Sons Ltd., 2011, pp. 39-53.

[12] E. Lassner and W.-D. Schubert, Tungsten: Properties, Chemistry, Technology of the Element, Alloys, and Chemical Compounds, New York: Springer US, 1999.

[13] J. Reiser, J. Hoffmann, U. Jäntsch, M. Klimenkov, S. Bonk, C. Bonnekoh, M. Rieth, A. Hoffmann and T. Mrotzek, "Ductilisation of tungsten (W): On the shift of the brittle-to-ductile transition (BDT) to lower temperatures through cold rolling," *International Journal of Refractory Metals and Hard Materials,* vol. 54, pp. 351-369, 2016.

[14] D. J. Palmer and P. G. Dickens, "Tungsten dioxide: structure refinement by powder neutron diffraction," *Acta Crystallographica Section B,* vol. 35, no. 9, pp. 2199-2201, 1979.

[15] H. T. Klippel, "The thermal response of the first wall of fusion reactor blanket to plasma disruptions," Netherlands Energy Research Foundation (ECN), 1983.

[16] C. Jonghyun, S. Hyun-Min, R. Ki-Baek, H. Seong-Hyeon, K. Gon-Ho and H. Heung Nam, “Fabrication of sintered tungsten by spark plasma sintering and investigation of thermal stability,” *In International Journal of Refractory Metals and Hard Materials,* vol. 69, pp. 164-169, 2017.